Opportunistic Spectrum Sharing with Multiple Cochannel Primary Transmitters

Ahmed O. Nasif and Brian L. Mark*
Dept. of Electrical and Computer Eng.
George Mason University
4400 University Drive, MS 1G5
Fairfax, VA 22030
tel: 703-993-4069, fax: 703-993-1601
email: { anasif , bmark }@gmu.edu

NAPL Technical Report: Feb. 20, 2009
Number: TR-GMU-NAPL-Y09-N1
GMU Network Architecture and Performance Laboratory (NAPL)

Abstract

We present a distributed, collaborative algorithm to enable opportunistic spectrum access for cognitive radios in the presence of multiple cochannel transmitters. A spectrum hole detection and estimation technique based on received signal strength observations is developed, which allows the coexistence of both licensed and unlicensed transmitters. We address the issues of how to perform collaborative spectrum sensing in the presence of multiple cochannel transmitters and how to determine the maximum transmit power that can be used for a given frequency channel by a cognitive radio while avoiding harmful interference to the licensed network. Simulation results are provided to validate the feasibility and performance of the proposed scheme.

Index Terms

Spectrum access, Spectrum sharing, Cognitive radio, Radio resource management, Collaboration, Geolocation, Cramér-Rao bound, Cochannel transmitters, Measurement clustering

Opportunistic Spectrum Sharing with Multiple Cochannel Primary Transmitters

Ahmed O. Nasif and Brian L. Mark

I. Introduction

Recently there has been much interest in cognitive radios (CRs) and its application to opportunistic spectrum access (OSA) to maximize the utilization of licensed spectrum [1], [2]. CRs equipped with features like frequency agility, high receiver sensitivity and location-awareness, are seen as a promising technology to allow the non-disruptive co-existence of unlicensed (secondary) users alongside the licensed (primary) users. Most of the proposed OSA schemes in the literature can be categorized into *coordinated* (the so called *property-rights* model) and *uncoordinated* (the so called *commons* model) frameworks [2]. In the coordinated approach, the primary and secondary nodes can exchange information and cooperatively increase spectrum utilization [3]. In uncoordinated OSA schemes, which is the model of interest for this paper, the primary is oblivious to the existence of secondary nodes, and the secondary system senses the activity of the primary system to opportunistically use the same spectrum, provided that no harmful interference is caused to the primary. In other words, the secondary system tries to fill the "spectrum holes", which may represent opportunities in time or in space or both.

OSA in the time domain has been studied extensively using the tools of information theory [4], game theory [5], queuing theory [6], and partially observable Markov chains [7]. Channel sensing mechanisms, detector design and effect of collaboration among secondary nodes have received considerable attention [8]–[10]. On the other hand, the use of location information and localization to exploit spatial spectrum holes have received relatively limited attention.

Localization for cognitive radio networks poses unique challenges, such as lack of coordination with the primary system and the need for robustness against a wide range of operating conditions. The enhancement of cognitive capabilities with location information, which can be utilized to perform dynamic spectrum management, network planning and handover is discussed in [11]. To ensure the operation of CRs under different environments, cognitive positioning system (CPS) based on time-of-arrival (TOA) is proposed in [12]. Localization using signal strength (SS) measurements of a primary transmitter with unknown transmit power based on constrained least squares approach is considered in [13]. Localization involving

multiple primary transmitters is studied in [14], [15], where it is assumed that the number of transmitters and the transmit power are known a priori. An experimental study, employing a triangulation-based heuristic approach for multiple transmitter localization using synchronized sensing is presented in [16]. Range-free localization of the primary is proposed in [17], while the use of spatial statistics to characterize CR networks is suggested in [18]. Many of the existing works on spatial spectrum sensing assume a single primary transmitter scenario and knowledge of the transmitter's location and transmit power [19]–[21].

A simple Listen-Before-Talk (LBT) algorithm is analyzed in [22], where the spectrum hole is characterized in terms of the *maximum interference-free transmit power* (MIFTP). The MIFTP is defined as the maximum power level at which a secondary node can transmit without causing harmful interference to the primary users. In [23], we proposed an approach to collaborative spectrum hole detection and estimation based on SS observations obtained by group of secondary nodes with respect to a single primary transmitter. In particular, an approximate expression for the MIFTP for a single secondary node was obtained. However, in various wireless systems, for example, cellular systems, one must consider the existence of multiple cochannel primary and secondary transmitters.

In an uncoordinated OSA scheme, the operation of the secondary system must appear transparent to the primary, and it is likely that the secondary may have only very limited a priori information about it. Particularly, the number of transmitters, their transmit powers and locations, are not assumed to be known a priori. In such a scenario, the secondary nodes can rely on collaboration among each other to sense the primary system. When multiple primary transmitters are present, the measurement used to sense the primary becomes more "noisy" due to cochannel interference, which may lead to secondary transmissions that cause harmful interference to the primary users. In such a model, the challenge is to characterize the primary transmitters using a collection of measurements taken by secondary nodes, and in the process also take into account the sensing error. In an infrastructureless network environment, it is highly desirable to have an approach to sense the primary transmitters in a distributed and iterative fashion, rather than having a computationally intensive centralized solution. Once the primary transmitters have been identified, the allowable transmit power or the MIFTP of the secondary nodes needs to be determined. Again, it is possible to pose this problem in a centralized formulation, akin to the traditional power control and power allocation schemes. But for decentralized applications, it is useful to find

the MIFTP in a distributed manner for the same reason mentioned above. In other words, a particular secondary node, using all the information of the cochannel transmitters, should be able to estimate its own MIFTP.

In this paper, we present a localization-based distributed approach to spatial sensing of the primary transmitters using SS measurements taken synchronously by secondary nodes. In our OSA model, a primary transmitter is characterized by its location and transmit power. Given a set of measurements, the first task is to identify the total number of cochannel primary transmitters and perform measurement clustering, so that the clustered secondary nodes can form groups and estimate the parameters of the primary transmitter in their vicinity, ignoring the effect of cochannel interference temporarily. Subsequently, the clustered groups can share the estimated parameters of the transmitters located in their vicinity with other groups to improve the initial estimates. This results in a distributed and iterative method to mitigate the effect of cochannel interference in spatial sensing. We show that spatial spectrum holes can be identified accurately provided that locally sensed information about cochannel transmitters is shared among the secondary nodes. In particular, we propose the maintenance of a distributed database, called the *T-map*, containing cochannel transmitter information including location, power, error estimates, and other information. Once all the parameters of the transmitters are estimated, a method using the T-map is proposed to determined the approximate MIFTP that can be allocated to a particular secondary node without causing harmful interference to the existing cochannel primary nodes.

The remainder of the paper is organized as follows. Section II, describes the OSA model in detail. Section III presents a collaborative and distributed localization-based spatial spectrum sensing scheme to mitigate cochannel interference. An approximation for the MIFTP in the presence of multiple transmitters is obtained in Section IV. Section V, presents some numerical results to validate the feasibility and performance of our proposed approach. Finally, the paper is concluded in Section VI.

II. Collaborative Spectrum Sharing Model

Consider a group of CRs deployed in the coverage area of a licensed network consisting of multiple primary transmitters operating on a given channel $\gamma_i \in \Gamma$, where Γ denotes the set of channels under consideration. We propose a collaborative OSA scheme that identifies the spatial regions where the CRs

can reuse the channel γ_i, without causing harmful interference to the primary receivers and to each other. In the literature, this is referred to as *spectrum hole discovery*. No direct communication between the primary and CR nodes is possible, but CRs can communicate with each other for robust spectrum sensing. Without loss of generality, we assume the existence of a common control channel that can be used by the CRs to exchange control information.

A. SS-based observation model

We assume that all transmissions are omnidirectional and the propagation model is homogeneous, with lognormal shadowing. The received SS at node i due to node j is denoted by

$$R_{ij} = s_j - g(d_{ij}) + W_{ij} \text{ [dBm]}, \tag{1}$$

where s_j is the transmit power of node j, $g(d_{ij})$ is the path loss between two nodes separated by d_{ij}, and $W_{ij} \sim \mathcal{N}(0, \sigma_W^2)$. Assume that $g(d)$ is continuous, monotonically increasing and invertible. In general, $g(\cdot)$ is also a function of path loss factor, antenna heights, antenna polarization, carrier frequency, terrain details etc., but for simplicity we assume that these other parameters can be estimated separately. Since multipath fast fading occurs on a much smaller time scale than shadowing, it is fair to assume that the fast fading can be practically eliminated by employing averaging (see [17], [24]). The net SS received at node i due to a set of cochannel transmitters $\mathcal{J}$ in dBm is given by

$$R_i = 10 \log_{10} \left(\sum_{j \in \mathcal{J}} 10^{\frac{R_{ij}}{10}} \right), \tag{2}$$

B. Definition of MIFTP

Denote the set of the cochannel primary transmitters and the secondary nodes by $\mathcal{P}$ and $\mathcal{A}$, respectively. Each node $a \in \mathcal{P} \cup \mathcal{A}$ has an associated location (x_a, y_a) and transmit power s_a. The primary receivers are referred to as *victim* nodes, since they can potentially be disrupted by secondary transmissions. The *coverage distance* of primary transmitter $p \in \mathcal{P}$ is given by

$$d_{\text{cov}}(p) = g^{-1} \left(s_p - r_{\min} + \sigma_W Q^{-1}(1 - \varepsilon_{\text{cov}}) \right), \tag{3}$$

where s_p is the transmit power of p, ε_{cov} is a predefined upper limit on the outage probability of an intended receiver located inside the coverage area of p, $r_{\min}$ is the detection threshold of primary receivers

(i.e., victims), $g^{-1}(\cdot)$ denotes the inverse of $g(\cdot)$ and $Q(x) \triangleq \frac{1}{\sqrt{2\pi}} \int_x^\infty e^{-\frac{t^2}{2}} dt$ denotes the standard Q-function (cf. [23]).

We define the *coverage region* of $p \in \mathcal{P}$ as the closed ball or disk centered at p with radius $d_{\text{cov}}(p)$, denoted by $\overline{B}_{\text{cov}}(p)$. The coverage region corresponds to the geographical area in which the received signal from p is sufficiently strong to satisfy a certain quality-of-service (QoS) requirement. Nodes residing within the coverage region are potential *victim* nodes, since they may be receiving transmissions from node p and may experience interference from cochannel secondary transmitters. Nodes outside the coverage region will be oblivious to interference caused by secondary transmissions. Similarly, all secondary nodes detecting the signal of a particular primary transmitter p, must be located within the *detection radius* $d_{\text{det}}(p)$, defined as

$$d_{\text{det}}(p) = g^{-1}(s_p - r_a + \sigma_W Q^{-1}(1 - \varepsilon_{\text{cov}})), \tag{4}$$

where r_a is the detection threshold of the secondary nodes.

Consider a set of existing cochannel secondary transmitters $\mathcal{A}_T \subset \mathcal{A}$ and a secondary node $b \in \mathcal{A} \setminus \mathcal{A}_T$ that is considering to reuse the same channel. Define $\mathcal{A}_0 \triangleq \mathcal{A}_T \cup \{b\}$. Denote by I_v, the aggregate interference power received at a victim node v due to the transmissions of nodes in $\mathcal{A}_0$. We ignore the effect of interference caused by cochannel primary transmitters. Typically, this would be taken into account in the design of the primary network. If this is not the case, we can simply treat the primary cochannel transmitters as secondary transmitters for the purpose of interference analysis. The *interference probability* with respect to v is defined as the probability that I_v exceeds a predefined threshold i_{max}:

$$P_{\text{int}}(\mathcal{A}_0, v) \triangleq \Pr\{I_v \geq i_{\text{max}}\}, \tag{5}$$

when each node $a \in \mathcal{A}_0$ is transmitting with power s_a. This threshold can be set to satisfy the interference tolerance policy of the primary system.

The objective of the proposed OSA scheme is to quantify the maximum interference-free transmit power (MIFTP) that can be allocated to secondary node b. The MIFTP for node b is defined as the maximum power that can be allocated to b such that the interference probability with respect to any potential victim node within the coverage distance of a transmitter $p \in \mathcal{P}$ does not exceed a threshold $\varepsilon_{\text{int}} > 0$, $\forall p \in \mathcal{P}$. More formally, the MIFTP for node b with respect to a single transmitter p can be

defined as follows (cf. [23]):

$$s_b^*(p) = \sup\{s_b : P_{\text{int}}(\mathcal{A}_0; s_b, x, y) \leq \varepsilon_{\text{int}}; \forall (x,y) \in \overline{B}_{\text{cov}}(p)\} \tag{6}$$

where the notation $P_{\text{int}}(\mathcal{A}_0; s_b, x, y)$ is meant to emphasize that the interference probability is a function of node b's transmit power s_b and the location (x, y) of a potential victim node v. The MIFTP of node b in the presence of the set of cochannel primary transmitters $\mathcal{P}$ is then given by $s_b^* \triangleq \min_{p\in\mathcal{P}} s_b^*(p)$.

C. T-map

In a network consisting of multiple cochannel transmitters, the parameter of interest is $\boldsymbol{\Theta} \triangleq \{\boldsymbol{\theta}_p, \forall p \in \mathcal{P} \cup \mathcal{A}_T\}$, with $\boldsymbol{\theta}_p \triangleq (x_p, y_p, s_p)$, where s_p is the transmit power of node p, located at (x_p, y_p). It is clear from (6) that in order to compute the MIFTP, it is necessary to estimate $\boldsymbol{\Theta}$. The presence of cochannel interference increases the error in estimating $\boldsymbol{\Theta}$, which can be mitigated if the secondary nodes share their estimates with other more distant secondary nodes (see Section III). Therefore, we propose the maintenance of a distributed database, called the *T-map*, containing relevant information about all cochannel transmitters.

In [23], it was shown that given a set of SS measurements, the maximum likelihood (ML) estimator is optimal in the mean-squared-error (MSE) sense and optimality is achieved as the observation noise becomes vanishingly small. The ML estimate (MLE) of the Cramer-Rao Bound (CRB) was found to provide an accurate approximation for the estimation error. Hence, we propose that the T-map store the MLEs of each transmitter's parameters and the associated CRBs:

$$\boldsymbol{T} \triangleq \left\{ \left(\hat{\boldsymbol{\theta}}_p, \hat{\boldsymbol{J}}_{\boldsymbol{\theta}_p}^{-1} \right), \forall p \in \mathcal{P} \right\} \cup \{\boldsymbol{\theta}_a, \forall a \in \mathcal{A}_T\}, \tag{7}$$

where $\hat{\boldsymbol{\theta}}_p$ is the MLE[1] of $\boldsymbol{\theta}_p$ and $\hat{\boldsymbol{J}}_{\boldsymbol{\theta}_p}^{-1}$ is the MLE of the associated CRB.

In general, the true parameters of some nodes in $\mathcal{A}_T$ may not be known. In this case, we treat these particular secondary transmitters as primary transmitters and estimate their corresponding unknown parameters. For a given frequency channel γ_i and time t_j, the T-map $\boldsymbol{T}_{i,j}$ characterizes the spatial region where secondary transmissions can be allowed. For a static set of primary transmitters, the T-map maintained by a secondary node should converge after a certain time period. In a dynamic scenario, the T-map should track changes that take place in the spectrum occupancy profile over time.

[1]Throughout this paper, all estimates indicated by ˆ represent MLEs.

III. Collaborative Sensing Scheme

To estimate the MIFTP, the secondary nodes must first update the T-map from their received SS measurements. This SS observation set is denoted by $\mathcal{O} \triangleq \{(R_a, \boldsymbol{L}_a) : a \in \mathcal{A}\}$, where R_a is the net SS received due to all cochannel transmitters at the secondary node a, located at $\boldsymbol{L}_a \triangleq (x_a \ y_a)$. In the proposed scheme, SS measurements are shared *locally* among neighboring nodes and localization estimates are shared *globally* via the T-map construct. Through collaborative information sharing, the T-map is maintained in a distributed fashion by means of networking protocols. Cochannel interference due to the primary transmitters introduces error in the SS measurements. For example, to localize node p, instead of $\{R_{ap} : a \in \mathcal{A}\}$ only $\{R_a : a \in \mathcal{A}\}$ can be observed, resulting in higher estimation error. This effect can be mitigated by sharing the estimates of the interfering primary transmitters among the secondary nodes via the T-map and by accounting for the associated cochannel interference. In the remainder of this section, we consider the case $M = 2$. Generalization of the approach to arbitrary M is straightforward.

A. With no information

Given a set of independent local observations $\mathcal{O}_1 \triangleq \{(R_a, \boldsymbol{L}_a) : a \in \mathcal{A}_1 \subset \mathcal{A}\}$ in the vicinity of a primary transmitter, say $p_1 \in \mathcal{P}$, the MLE of the parameter $\boldsymbol{\theta}_1 \triangleq [x_{p_1} \ y_{p_1} \ s_{p_1}]^T$ can be found. In the absence of any information about other cochannel transmitters, the log-likelihood function has the following form [23]:

$$F_{1A}(\boldsymbol{\theta}_1) \triangleq \sum_{a \in \mathcal{A}_1} \ln f_{R_a|\boldsymbol{\theta}_1}, \tag{8}$$

where $R_a|\boldsymbol{\theta}_1 \sim \mathcal{N}(s_{p_1} - g(d_{ap_1}), \sigma_W^2)$. The MLE is found by solving the optimization problem $\hat{\boldsymbol{\theta}}_{1A} = \arg\max_{\boldsymbol{\theta}_1} \ F_{1A}(\boldsymbol{\theta}_1)$.

B. With true information

If the *true* parameter $\boldsymbol{\theta}_2 \triangleq [x_{p_2} \ y_{p_2} \ s_{p_2}]^T$, of another cochannel transmitter p_2, is known, the observations in $\mathcal{O}_1$ can be modeled as

$$R_a = 10 \log_{10} \left(10^{\frac{R_{ap_1}}{10}} + 10^{\frac{R_{ap_2}}{10}} \right) = \kappa^{-1} \ln \left(e^{\kappa R_{ap_1}} + e^{\kappa R_{ap_2}} \right),$$

where $\kappa \triangleq \frac{\ln 10}{10}$. Approximating the sum of independent lognormal random variables by another lognormal [25], yields $R_a|\boldsymbol{\theta}_1, \boldsymbol{\theta}_2 \sim \mathcal{N}(\frac{\mu_{Ba}}{\kappa}, \frac{\sigma^2_{Ba}}{\kappa^2})$, where

$$\mu_{Ba} \triangleq \ln(k_1) - \frac{\sigma^2_{Ba}}{2}, \quad \sigma^2_{Ba} \triangleq \ln\left(1 + \frac{k_2^2}{k_1^2}\right), \tag{9}$$

$$k_1 \triangleq e^{\frac{\kappa^2\sigma_W^2}{2}}\left(e^{\kappa u_{ap_1}} + e^{\kappa u_{ap_2}}\right), \quad k_2^2 \triangleq e^{\kappa^2\sigma_W^2}\left(e^{\kappa^2\sigma_W^2} - 1\right)\left(e^{2\kappa u_{ap_1}} + e^{2\kappa u_{ap_2}}\right), \tag{10}$$

and $u_{ij} \triangleq s_j - g(d_{ij})$. Note that u_{ap_2} is known and $\boldsymbol{\theta}_1$ is the only unknown. The log-likelihood function is $F_{1B}(\boldsymbol{\theta}_1) \triangleq \sum_{a\in\mathcal{A}_1} \ln f_{R_a|\boldsymbol{\theta}_1,\boldsymbol{\theta}_2}$, and the ML solution is given by $\hat{\boldsymbol{\theta}}_{1B}(\boldsymbol{\theta}_1) = \arg\max_{\boldsymbol{\theta}_1} \; F_{1B}(\boldsymbol{\theta}_1)$. We have observed (see Fig. 1) that in the region of practical interest, $u_{ap_i} \in [-150, 100]$ dBm, $\sigma_{Ba} \lesssim \kappa\sigma_W, \forall a$, where $x_1 \lesssim x_2$ means that x_1 is upper bounded by x_2 which is not too far from x_1. If the observations R_a are scaled as $\widetilde{R}_a = \kappa R_a$, this approximation can be used to obtain an equivalent but simpler objective function compared to $F_{1B}(\boldsymbol{\theta}_1)$. In this case, we have $\hat{\boldsymbol{\theta}}_{1B} = \arg\max_{\boldsymbol{\theta}_1} \; \widetilde{F}_{1B}(\boldsymbol{\theta}_1)$, where

$$\widetilde{F}_{1B}(\boldsymbol{\theta}_1) \triangleq \sum_{a\in\mathcal{A}_1} \ln f_{\widetilde{R}_a|\boldsymbol{\theta}_1,\boldsymbol{\theta}_2}, \tag{11}$$

and $\widetilde{R}_a|\boldsymbol{\theta}_1, \boldsymbol{\theta}_2 \sim \mathcal{N}\left(\ln\left(\sum_{i=1,2} e^{\kappa u_{ap_i}}\right), \kappa^2\sigma_W^2\right)$.

C. With estimated information

In many cases, only the *estimated* information about other cochannel transmitters is available, via the distributed maintenance of the T-map. Assume that the ML estimated parameters $(\hat{\boldsymbol{\theta}}_2, \hat{\boldsymbol{J}}^{-1}_{\boldsymbol{\theta}_2})$ of transmitter p_2 are known. Note that here $\hat{\boldsymbol{\theta}}_2$ is found by solving the likelihood function F_{2A} corresponding to p_2 (similar to F_{1A}), i.e., $\hat{\boldsymbol{\theta}}_2 \equiv \hat{\boldsymbol{\theta}}_{2A}$ and $\hat{\boldsymbol{J}}^{-1}_{\boldsymbol{\theta}_2} \equiv \hat{\boldsymbol{J}}^{-1}_{\boldsymbol{\theta}_{2A}}$. Instead of u_{ap_2}, we can obtain $\hat{u}_{ap_2}$, where $\hat{u}_{ap_2} \triangleq \hat{S}_{p_2} - g(\hat{D}_{ap_2})$ denotes the MLE of u_{ap_2} and $\hat{\boldsymbol{\theta}}_2 = [\hat{X}_{p_2}\ \hat{Y}_{p_2}\ \hat{S}_{p_2}]^T$ denotes the MLE of $\boldsymbol{\theta}_2$, via the invariance principle (cf. [26, p. 217]), which states that the MLE of a function $q(\cdot)$ of $\boldsymbol{\Phi}$ is given by $q(\hat{\boldsymbol{\Phi}})$, where $\hat{\boldsymbol{\Phi}}$ denotes the MLE of $\boldsymbol{\Phi}$. Since the MLE of the CRB approaches the estimation error as $\sigma_W \to 0$ [27], we propose the following model for R_{ap_2}:

$$R_{ap_2} = u_{ap_2} + W_{ap_2} = \hat{u}_{ap_2} + W_{2a} + W_{ap_2},$$

where $W_{2a} \sim \mathcal{N}(0, \hat{\sigma}^2_{2a})$ with $\hat{\sigma}^2_{2a} \triangleq \hat{\boldsymbol{H}}_a^T \hat{\boldsymbol{J}}^{-1}_{\boldsymbol{\theta}_2} \hat{\boldsymbol{H}}_a$. Again, $\hat{\boldsymbol{H}}_a$ is the MLE of $\boldsymbol{H}_a$ where

$$\boldsymbol{H}_a \triangleq \left[\frac{\partial u_{ap_2}}{\partial x_{p_2}}, \frac{\partial u_{ap_2}}{\partial y_{p_2}}, \frac{\partial u_{ap_2}}{\partial s_{p_2}}\right]^T = \left[-\dot{g}(d_{ap_2})\cos\phi_{ap_2}, -\dot{g}(d_{ap_2})\sin\phi_{ap_2}, 1\right]^T, \tag{12}$$

and $\dot{g}(d) \triangleq \frac{\partial g(d)}{\partial d}$. Hence, $R_{ap_2}|\hat{\boldsymbol{\theta}}_2 \sim \mathcal{N}(\hat{u}_{ap_2}, \hat{\sigma}_{2a}^2 + \sigma_W^2)$ and $R_a|\boldsymbol{\theta}_1, \hat{\boldsymbol{\theta}}_2 \sim \mathcal{N}(\frac{\mu_{Ca}}{\kappa}, \frac{\sigma_{Ca}^2}{\kappa^2})$, where

$$\mu_{Ca} \triangleq \ln(k_3) - \frac{\sigma_{Ca}^2}{2}, \quad \sigma_{Ca}^2 \triangleq \ln\left(1 + \frac{k_4^2}{k_3^2}\right), \quad k_3 \triangleq e^{\frac{\kappa^2\sigma_W^2}{2}}\left(e^{\kappa u_{ap_1}} + e^{\kappa\hat{u}_{ap_2} + \frac{\kappa^2\hat{\sigma}_{2a}^2}{2}}\right),$$

$$k_4^2 \triangleq \left(e^{\kappa^2\sigma_W^2} - 1\right)e^{2\kappa u_{ap_1} + \kappa^2\sigma_W^2} + \left(e^{\kappa^2\hat{\sigma}_{2a}^2 + \kappa^2\sigma_W^2} - 1\right)e^{2\kappa\hat{u}_{ap_2} + \kappa^2\hat{\sigma}_{2a}^2 + \kappa^2\sigma_W^2}.$$

The corresponding log-likelihood function is $F_{1C}(\boldsymbol{\theta}_1) \triangleq \sum_{a\in\mathcal{A}_1} \ln f_{R_a|\boldsymbol{\theta}_1,\hat{\boldsymbol{\theta}}_2}$, and the ML solution is given by $\hat{\boldsymbol{\theta}}_{1C} = \arg\max_{\boldsymbol{\theta}_1} \quad F_{1C}(\boldsymbol{\theta}_1)$. Similar to Section III-B, to simplify the objective function we can use the scaled observations to solve $\hat{\boldsymbol{\theta}}_{1C} = \arg\max_{\boldsymbol{\theta}_1} \quad \widetilde{F}_{1C}(\boldsymbol{\theta}_1)$, where

$$\widetilde{F}_{1C}(\boldsymbol{\theta}_1) \triangleq \sum_{a\in\mathcal{A}_1} \ln f_{\widetilde{R}_a|\boldsymbol{\theta}_1,\hat{\boldsymbol{\theta}}_2}, \tag{13}$$

and $\widetilde{R}_a|\boldsymbol{\theta}_1, \hat{\boldsymbol{\theta}}_2 \sim \mathcal{N}\left(\ln\left(e^{\kappa u_{ap_1}} + e^{\kappa\hat{u}_{ap_2} + \frac{\kappa^2\hat{\sigma}_{2a}^2}{2}}\right), \kappa^2\sigma_W^2\right)$. Note that $\hat{\boldsymbol{\theta}}_{1C} \to \hat{\boldsymbol{\theta}}_{1B}$, as $\sigma_{2a} \to 0, \forall a$. Our hypothesis is that $\hat{\boldsymbol{\theta}}_{1B}$ and $\hat{\boldsymbol{\theta}}_{1C}$ are better estimators than $\hat{\boldsymbol{\theta}}_{1A}$ in terms of mitigating the error induced by cochannel interference. The effectiveness of this proposed collaborative sensing strategy is studied numerically in Section V. The CRBs corresponding to $\hat{\boldsymbol{\theta}}_{1B}$ and $\hat{\boldsymbol{\theta}}_{1C}$ for arbitrary M are derived in [28].

D. Measurement clustering and collaborative sensing

When multiple cochannel transmitters are present, accurate localization depends on using an appropriate set of SS measurements. More precisely, as stated in Section III, the measurements should be shared locally among neighboring CRs. For locating a particular transmitter, the most useful measurements are received by nodes residing in its vicinity. This is because the effect of cochannel interference on these measurements is expected to be small. On the other hand, the worst measurements are the ones which have equal contribution of received power from multiple transmitters. Since it is difficult to resolve the power contribution from each transmitter, a large error in localization can be incurred in this case. So, it is important to collect measurements that have the strongest contribution from a particular transmitter. This is equivalent to assigning each measurement to the transmitter closest to it. Therefore, to minimize the effect of cochannel interference, all the measurements should be *clustered* appropriately, where each measurement cluster represents the subset of measurements to be used in the localization of a particular transmitter.

In [29], two schemes for measurement clustering, one based on minimum description length (cf. [30]) and the other based on minimum mean square error, are proposed. Both schemes produce an estimate, $\hat{M}$,

of the number of cochannel transmitters, together with an associated set of *initial* parameter estimates, $\{\hat{\boldsymbol{\theta}}_i\}_{i=1}^{\hat{M}}$, which is most likely to have generated the given set of measurements. The measurements are then assigned to the nearest estimated transmitter from $\{\hat{\boldsymbol{\theta}}_i\}_{i=1}^{\hat{M}}$.

Once the initial estimates are found via measurement clustering, the effect of cochannel interference can be mitigated using the approach discussed in Section III-C. In particular, note that $\hat{\boldsymbol{\theta}}_{1C}$ is a better estimator than $\hat{\boldsymbol{\theta}}_{1A}$ (in terms of MSE), since it uses the information of $\hat{\boldsymbol{\theta}}_2$, (cf. [28]). Symbolically, we denote this by $\hat{\boldsymbol{\theta}}_{1A} \overset{\hat{\boldsymbol{\theta}}_2}{\rightarrow} \hat{\boldsymbol{\theta}}_{1C}$. The corresponding *compensation* for $\hat{\boldsymbol{\theta}}_2$ is given by $\hat{\boldsymbol{\theta}}_2 \overset{\hat{\boldsymbol{\theta}}_{1C}}{\rightarrow} \hat{\boldsymbol{\theta}}_{2C}$, where $\hat{\boldsymbol{\theta}}_{2C}$ denotes the modified estimator of $\hat{\boldsymbol{\theta}}_2$ incorporating the knowledge of $\hat{\boldsymbol{\theta}}_{1C}$. We can continue the procedure as $\hat{\boldsymbol{\theta}}_{1C} \overset{\hat{\boldsymbol{\theta}}_{2C}}{\rightarrow} \hat{\boldsymbol{\theta}}_{1C}^{'}$, then $\hat{\boldsymbol{\theta}}_{2C} \overset{\hat{\boldsymbol{\theta}}_{1C}^{'}}{\rightarrow} \hat{\boldsymbol{\theta}}_{2C}^{'}$, and so on. Therefore, a simple convergence criterion is needed to halt the recursive procedure, which justifies the tradeoff between accuracy improvement and computational load. For example, the rule may simply be to stop when the difference between successive iterations is sufficiently small.

IV. Maximum Interference-Free Transmit Power

Consider the problem of calculating the MIFTP for the secondary node $b \in \mathcal{A} \setminus \mathcal{A}_T$ (see (6)). In this section, we first formulate an approach to compute the true MIFTP and then discuss a practical method for obtaining an approximation to the MIFTP.

A. True MIFTP calculation

An expression of the interference probability is given as follows (see Appendix B for a proof).

Proposition 1: The interference probability at victim node v due to nodes in $\mathcal{A}_0$ is given by

$$P_{\text{int}}(\mathcal{A}_0; s_b, v) = Q\left(\frac{\kappa i_{\max} - \mu}{\sigma}\right), \tag{14}$$

where

$$\mu \triangleq \frac{\kappa^2\sigma_W^2}{2} - \frac{\sigma^2}{2} + h, \quad \sigma^2 \triangleq \ln\left(1 + \frac{k_6^2}{k_5^2}\right), \quad h \triangleq \ln\left(\frac{e^{\kappa s_b(p)}}{e^{\kappa g(d_{vb})} + \sum_{a\in\mathcal{A}_T} \frac{e^{\kappa s_a}}{e^{\kappa g(d_{va})}}}\right), \tag{15}$$

$$k_5 \triangleq e^{\frac{\kappa^2\sigma_W^2}{2}+h}, \qquad k_6^2 \triangleq e^{\kappa^2\sigma_W^2}\left(e^{\kappa^2\sigma_W^2} - 1\right)\left(L_b^2 + \sum_{a\in\mathcal{A}_T} L_a^2\right). \tag{16}$$

The interference probability at victim v depends on three quantities: (i) the interference tolerance threshold, $i_{\max}$, (ii) the variance of the shadowing noise, σ_W^2, and (iii) the aggregate interference power, h, received at v. The following lemma provides a method for computing the MIFTP.

Lemma 1: For a secondary node b such that $(x_b, y_b) \notin \overline{B}_{\rm cov}(p)$ the MIFTP with respect to primary transmitter $p \in \mathcal{P}$ is given by

$$s_b^*(p) = \min_{(x,y)\in\overline{B}_{\rm cov}(p)} s_b^*(p; x, y), \tag{17}$$

where

$$s_b^*(p; x, y) \triangleq \max\{s_b : P_{\rm int}(\mathcal{A}_0; s_b, x, y) \le \varepsilon_{\rm int}\}. \tag{18}$$

The complexity of the optimization problem suggested by Lemma 1 can be reduced by restricting the minimization problem to the boundary of the coverage region $\overline{B}_{\rm cov}(p)$ as stated in the next proposition (see Appendix C for a proof).

Proposition 2: Given a set of secondary cochannel transmitters with parameters $\{\boldsymbol{\theta}_a\} = \{(x_a, y_a, s_a)\}$, all located outside the coverage region $\overline{B}_{\rm cov}(p)$, the maximum interference due to path loss alone is achieved on the boundary $\partial B(p)$, i.e., the circle centered at p with radius $d_{\rm cov}(p)$.

Combining Lemma 1 and Proposition 2 simplifies the computation of MIFTP (see Appendix D for a proof).

Corollary 1:

$$s_b^*(p) = \min_{(x,y)\in\partial B_{\rm cov}(p)} s_b^*(p; x, y) = \min_{\psi\in[0,2\pi)} s_b^*(p; x_p(\psi), y_p(\psi)) \tag{19}$$

with $s_b^*(p; x, y)$ defined in (18), and

$$x_p(\psi) \triangleq x_p + d_{\rm cov}(p)\cos\psi, \quad y_p(\psi) \triangleq y_p + d_{\rm cov}(p)\sin\psi. \tag{20}$$

The true MIFTP as defined in Lemma 1 or Corollary 1 cannot be calculated directly, since the T-map provides only $\{\hat{\boldsymbol{\theta}}_p, \hat{\boldsymbol{J}}_{\boldsymbol{\theta}_p}^{-1} : p \in \mathcal{P}\}$ and $\{\boldsymbol{\theta}_a : a \in \mathcal{A}_T\}$. Therefore, we develop an approximation to the MIFTP of b with respect to $p \in \mathcal{P}$ by first estimating the *critical distance*, $\hat{D}_b^*(p)$ to detect the presence of a spectrum hole. Then, an estimate, $\hat{s}_b^*(p)$, for the MIFTP is obtained by considering potential victim nodes lying on the circle $\partial B_{\rm cov}(p)$.

B. Critical distance estimate, $\hat{D}_b^*(p)$, and spectrum hole detection

For a particular $p \in \mathcal{P}$, the *critical distance estimate* with respect to node b is given by

$$\begin{aligned}\hat{D}_b(p) &\triangleq \hat{D}_{pb} - \hat{D}_{\rm cov}(p) \\ &\overset{(3)}{=} \sqrt{(\hat{X}_p - x_b)^2 + (\hat{Y}_p - y_b)^2} - g^{-1}(\hat{S}_p - r_{\min} + \sigma_W Q^{-1}(1 - \varepsilon_{\rm cov})),\end{aligned}$$

where $\hat{D}_{pb}$ and $\hat{D}_{\text{cov}}(p)$ denote the MLEs of d_{pb} and $d_{\text{cov}}(p)$, respectively. In the asymptotic regime $\sigma_W \to 0$,

$$E_p \triangleq \hat{D}_b(p) - d_b(p) = \hat{D}_{pb} - d_{pb} - (\hat{D}_{\text{cov}}(p) - d_{\text{cov}}(p))$$

can be modeled as $E_p \sim \mathcal{N}(0, \hat{J}_{pb}^{-1})$, where $\hat{J}_{pb}^{-1}$ denotes the MLE of the CRB corresponding to the error in estimating $\hat{D}_b(p)$, [27, Proposition 6]. Suppose $E_p = r$ and $\hat{D}_b(p) = r_0$. If $|r| \geq r_0 > 0$, then in the worst case, node b lies within $d_{\text{cov}}(p)$ of primary transmitter p. In this scenario, node b must not transmit, i.e., $s_b^* = -\infty$, to avoid potentially harmful interference to the victim nodes. If $0 < |r| < r_0$, then b can transmit, i.e., $s_b^* \neq -\infty$. Since we do not know r, we can only ensure that for the given realization $\hat{D}_b(p) = r_0 > 0$, the event $\{|E_p| < r_0\}$ occurs with high probability. In particular, for $s_b^* \neq -\infty$ and $\varepsilon \in (0, 1)$, we require $r_0 > \hat{R}^* > 0$, where

$$R^* \triangleq \min\{R : \Pr(|E_p| < R) \geq \varepsilon\} = \sqrt{\hat{J}_{pb}^{-1}} \cdot Q^{-1}\left(\frac{1-\varepsilon}{2}\right).$$

For example, for $\varepsilon = 0.9973$, $\hat{R}^* \approx 3\sqrt{\hat{J}_{pb}^{-1}}$. Define the set $\mathcal{D} \triangleq \left\{p \in \mathcal{P} : \hat{D}_b(p) \leq \hat{R}^*\right\}$. Whenever, $\mathcal{D} = \emptyset$, a spectrum hole with respect to b is detected, and the approximate MIFTP, $\hat{s}_b^*$ should be computed.

C. Interference probability and MIFTP approximation

An upper bound on $P_{\text{int}}(\mathcal{A}_0, v)$ is given by the following proposition. See Appendix E for a proof.

Proposition 3: The interference probability $P_{\text{int}}(\mathcal{A}_0, v)$ at a particular victim v located at (x_v, y_v) can be upper bounded by $Q(\gamma)$, where $\gamma \triangleq \frac{\kappa i_{\max} - \frac{\kappa^2\sigma_W^2}{2} + \frac{\sigma^2}{2} - h}{\kappa\sigma_W}$.

Define $F(\gamma) \triangleq \hat{\Gamma} - \gamma$, where $\hat{\Gamma}$ denotes the MLE of γ. Note that γ is a function of $\boldsymbol{\theta}_p$. Under some regularity conditions [26, p. 229], the CRBs of $\boldsymbol{\theta}_p$ and γ are related as $J_\gamma^{-1} = \boldsymbol{H}_0^T \boldsymbol{J}_{\boldsymbol{\theta}_p}^{-1} \boldsymbol{H}_0$, where $\boldsymbol{H}_0 \triangleq \left[\frac{\partial\gamma}{\partial x_p} \ \frac{\partial\gamma}{\partial y_p} \ \frac{\partial\gamma}{\partial s_p}\right]^T$ and is evaluated in [28]. In [23], we provide a closed-form expression of $\boldsymbol{J}_{\boldsymbol{\theta}_p}^{-1}$ and show that it is achievable as $\sigma_W \to 0$. It can be shown that if $\boldsymbol{J}_{\boldsymbol{\theta}_p}^{-1}$ is achievable asymptotically as $\sigma_W \to 0$, then so is J_γ^{-1}, (cf. [27, Proposition 4]). This means that in the asymptotic regime $F(\gamma) \sim \mathcal{N}(0, J_\gamma^{-1})$. Suppose for a particular realization $F(\gamma) = x$ and $\hat{\Gamma} = \hat{\gamma}$. Then, the upper bound on the interference probability conditioned on $F(\gamma) = x$ is given by $Q(\hat{\gamma} - x)$. Using the total probability theorem

$$\int_{-\infty}^{\infty} Q(\hat{\gamma} - x)\mathcal{N}(0, J_\gamma^{-1})dx = Q\left(\frac{\hat{\gamma}}{\sqrt{1 + J_\gamma^{-1}}}\right) \leq \frac{1}{2} e^{-\frac{\hat{\gamma}^2}{2\left(1 + J_\gamma^{-1}\right)}} \triangleq w(s_b, x, y), \tag{21}$$

where the first equality is obtained using a result in [31, p. 102] and the upper bound is valid for $\hat{\gamma} \geq 0$. We propose to approximate the MIFTP in terms of this upper bound[2] w on the interference probability averaged over all possible estimation errors. Since J_{γ}^{-1} is unknown, using the invariance principle we replace it by its MLE, $\hat{J}_{\gamma}^{-1}$, and denote the expression corresponding to (21) by $\hat{w}(s_b, x, y)$. In a manner analogous to Corollary 1, an approximation to the MIFTP can be computed as follows:

$$\hat{s}_b^*(p) \triangleq \min_{\psi \in [0, 2\pi)} \hat{s}_b^*(p; \hat{X}_p(\psi), \hat{Y}_p(\psi)), \tag{22}$$

where

$$\hat{X}_p(\psi) \triangleq \hat{X}_p + \hat{D}_{\text{cov}}(p) \cos\psi, \quad \hat{Y}_p(\psi) \triangleq \hat{Y}_p + \hat{D}_{\text{cov}}(p) \sin\psi, \tag{23}$$

$$\hat{s}_b^*(p; x, y) \triangleq \max\{s_b : \hat{w}(s_b, x, y) \leq \varepsilon_{\text{int}}\}. \tag{24}$$

A computationally simpler approximation to MIFTP can be obtained by assuming that the worst-case victim, say v^*, lies at the intersection of the circle $\partial B_{\text{cov}}(p)$ and the straight line connecting (x_b, y_b) and $(\hat{X}_p, \hat{Y}_p)$.

$$\hat{s}_b^*(p) = \max\{s_b : \hat{w}(s_b, x_{v^*}, y_{v^*}) \leq \varepsilon_{\text{int}}\}. \tag{25}$$

This is an one-dimensional search problem which is computationally less demanding than the two-step optimization problem given by (22) and (24). Numerical results presented in Section V suggest that this approximation is sufficiently accurate for practical scenarios.

We remark that localization accuracy is incorporated into above MIFTP approximations via the CRB term, J_{γ}^{-1}. In particular, as the estimation error increases, the MIFTP becomes more conservative, ensuring that the interference tolerance threshold, $i_{\max}$ is met, but also making the OSA scheme less efficient. This property of being conservative is important since secondary transmissions should do no harm to the primary system.

V. Numerical Results

For the numerical results presented in this section, we choose system parameter values that reflect the application of OSA to digital TV broadcast bands. The SS measurements are generated using the

[2]If, for any realization $\hat{\gamma} < 0$, we can use $Q\left(\frac{\hat{\gamma}}{\sqrt{1+J_{\gamma}^{-1}}}\right)$ to compute the MIFTP.

generic path loss function $g(d) = 10\epsilon \log_{10}(d)$, where d is distance and ϵ is the path loss exponent. Unless otherwise specified, all simulations are performed with the following parameter values: detection threshold for victims $r_{\text{min}} = -85$ dBm, detection threshold for secondary nodes $r_a = -90$ dBm, interference tolerance threshold $i_{\text{max}} = -100$ dBm, outage probability upper limit $\varepsilon_{\text{cov}} = 0.01$, allowable interference probability upper limit to victims $\varepsilon_{\text{int}} = 0.01$, shadowing standard deviation $\sigma_W = 8$ dB and path loss exponent $\epsilon = 4$. For a particular primary transmitter p and for each simulation trial, we randomly place N secondary nodes, with uniform distribution inside the coverage region $\overline{B}_{\text{cov}}(p)$. These nodes perform localization of p by evaluating the MLEs $(\hat{\boldsymbol{\theta}}_p, \hat{\boldsymbol{J}}_{\boldsymbol{\theta}_p}^{-1})$ (cf. [27]). Each result is averaged over K trials and shown with the associated 95% confidence interval, which arises due to randomness in the localizing node positions, as well as the shadowing noise.

A. Mitigation of cochannel interference

Consider two cochannel primary transmitters p_1 and p_2 parameterized by $(8, 0, 80)$ and $(0, 0, 80)$, respectively, where the first two numbers of the 3-tuple indicate location and the last number indicates transmit power with units of $[\text{km}, \text{km}, \text{dBm}]$. For these parameter values, $d_{\text{cov}}(p_1) = d_{\text{cov}}(p_2) = 4.6$ km and $d_{\text{det}}(p_1) = d_{\text{det}}(p_2) = 6.1$ km, (cf. (3) and (4)). Each measurement is generated by averaging over 100 raw measurements to reduce the effect of shadowing noise. We are interested in estimating $\boldsymbol{\theta}_1 = [x_{p_1}\ y_{p_1}\ s_{p_1}]^T$. To evaluate the performance of our proposed scheme, we find the ML solutions of the likelihood functions F_{1A}, $\widetilde{F}_{1B}$ and $\widetilde{F}_{1C}$ corresponding to (8), (11) and (13), respectively. As a performance measure, we calculate the mean *missed distance* (m), $\mathcal{E}_1 \triangleq \frac{1}{K}\sum_{i=1}^{K}\sqrt{(\hat{X}_{p_1}(i) - x_{p_1})^2 + (\hat{Y}_{p_1}(i) - y_{p_1})^2}$, over $K = 1000$ independent trials. In Fig. 2, we plot $\mathcal{E}_1$ as a function of the number of measurements. The bottom three curves correspond to measurements taken by secondary nodes located uniformly inside the circle with radius $d_{\text{det}}(p_1)$ centered at p_1. We observe that although the difference between Cases B and C is negligible, both cases show some improvement (≥ 50 m) over Case A. The top three curves correspond to the worst-case scenario where the measurements are taken by secondary nodes located only at the intersection of the detection regions $d_{\text{det}}(p_1)$ and $d_{\text{det}}(p_2)$. A significant accuracy improvement is seen in Cases B and C (≥ 335 m), more so in B than in C, over Case A. The improvement for the worst-case scenario is much greater because the proposed *compensation* becomes more prominent when

both transmitters contribute approximately equally to the measurements.

B. MIFTP vs. distance, d_{bp}

Now consider the following configuration of cochannel transmitters: $\boldsymbol{\theta}_p = (0, 0, 80)$, $\boldsymbol{\theta}_{a_1} = (20, 20, 40)$ and $\boldsymbol{\theta}_{a_2} = (-20, 20, 40)$. We vary the position, $(0, y_b)$ [km,km], of the test node b, where y_b ranges from 20 to 100 in increments of 10. The MIFTP of node b is computed according to the approach presented in Section IV. The angle ψ in (22) and (19) is discretized in increments of $\Delta\psi = \frac{\pi}{18}$ [rad]. Then the true MIFTP is computed according to (19). To approximate the MIFTP, $\mathcal{D}$ is computed for each trial. If $\mathcal{D} = 1$, then the MIFTP estimate is set to -174 dBm (which is the thermal noise floor at 1 Hz bandwidth at room temperature), otherwise, the estimated MIFTP is computed using (25). Note computation of the true MIFTP requires the solution of $N_T = 1 + \frac{2\pi}{\Delta\psi}$ one-dimensional optimization problems in (19), whereas for the proposed approximation approach given in (25) requires only one.

In Fig. 4, we plot the true and estimated MIFTP as a function of the distance d_{bp}. As expected, the estimated MIFTP increases with distance, but is always smaller than the true MIFTP. Although for $N = 4$ the estimation is extremely conservative, a considerable improvement is seen when $N = 6$. Using more measurements is only useful for distances smaller than 50 km. On average, the estimated values are smaller than the true value by 5.35 dB, when $N = 6$ for all distances. We also plot the average interference probability (cf. (19)) perceived by victim nodes in $\overline{B}_{\text{cov}}(p)$ when node b transmits at $\hat{s}_b^*(p)$ for $d_{bp} = 20$ km and $N = 6$. As shown in Fig. 5, the interference probability surface is always less than the specified upper bound $\varepsilon_{\text{int}} = 0.01$. The same has been observed for the values of d_{bp} as well. Thus, the proposed MIFTP approximation can be safely be used for opportunistic spatial spectrum access.

To study the effect of multiple primary transmitters, we consider the existence of another primary transmitter, p', in addition to p on the same channel and time, with $\boldsymbol{\theta}_{p'} = (0, 120, 80)$. Since the two transmitters are very far apart (120 km), we can ignore the effect of cochannel interference on localization. The true and approximate MIFTPs are calculated as $s_b^* = \min\{s_b^*(p), s_b^*(p')\}$ and $\hat{s}_b^* = \min\{\hat{s}_b^*(p), \hat{s}_b^*(p')\}$, respectively. Fig. 6 shows the variation of MIFTP as a function of distance. As node b moves away from transmitter p its MIFTP increases up to a certain level, then it decreases as it approaches transmitter p'.

C. MIFTP vs. shadowing noise, σ_W and interference probability threshold, ε_{int}

We set $d_{bt} = 40$ km and in Fig. 7 plot the estimated MIFTP as a function of the shadowing noise standard deviation, σ_W. As anticipated, the MIFTP decreases with increasing noise. This is because as the noise power increases, the localization error and the associated CRB increases, which in turn makes the MIFTP more conservative. For $N = 4$ the estimated values are very loose, but it can be made reasonably tight using $N = 6$ for any $\sigma_W \leq 9$ dB. Note that the decrease in true MIFTP is linear for all σ_W, but for the estimated MIFTP it is approximately linear only for $\sigma_W \leq 9$ dB. For the extreme case of $\sigma_W > 9$ dB, the estimated MIFTP is very loose and increasing N helps very little. In Fig. 8, we set $\sigma_W = 8$ dB and vary ε_{int}. We notice that as expected, the MIFTP becomes more conservative as the imposed interference constraint becomes tighter (lower ε_{int}). For $N \geq 6$, on average the estimated MIFTP is within 2.7 dB of the true value.

D. T-map and spectrum hole harvesting

Consider the node configuration of Fig. 4. For this case Fig. 9 shows a pictorial illustration of the T-map for a particular channel. In this example, the estimated parameters $\hat{\boldsymbol{\theta}}_t$ of primary transmitters t and are available, while the true parameters $\boldsymbol{\theta}_{a_1}$ and $\boldsymbol{\theta}_{a_2}$ of existing secondary transmitters a_1 and a_2 are also known. All these parameters along with the appropriate CRB estimates are contained in the T-map and are propagated throughout the secondary network via a collaborative network protocol.

The circles around t, a_1 and a_2 represent their respective (estimated or true) coverage regions. The circle centered at t represents C_t, inside which potential victim nodes reside. Given the information contained in the T-map, by computing $\mathcal{D}$ (see Section IV-B) node b can detect whether it is located inside a spectrum hole. If $\mathcal{D} = 0$, node b can compute its MIFTP using the approximation presented in Section IV-C. The circle centered at node b represents its coverage area when it transmits at its MIFTP estimate $\hat{s}_b^*(t)$. As node b moves away from t the size of its perceived spectrum hole increases, which it can fill up by transmitting at higher transmit powers specified by its MIFTP. Hence, the information contained in the T-map characterizes the location and size of the available spectrum holes in the spatial domain.

VI. Conclusion

We presented a collaborative OSA scheme whereby multiple primary and secondary transmitters can co-exist in an interference-free condition. We proposed a scheme of distributed sensing of the primary transmitters via the notion of a T-map, a distributed databased containing location, power, and error estimates of cochannel nodes. The MDL (Maximum Description Length) criterion is employed to identify the total number of cochannel transmitters in the network, and once this is determined, measurements closest to a particular transmitter are clustered together. Based on these clustered measurements, secondary nodes estimate the power and location of primary transmitters that are located in their vicinity. The effect of cochannel interference in localization is initially ignored and is later taken into account when global information about other cochannel transmitters becomes available via the T-map. Our approach to spatial OSA can be summarized symbolically as:

$$\mathcal{O} \underset{\text{clustering}}{\overset{\text{MDL}}{\longrightarrow}} \{\hat{\boldsymbol{\theta}}_t\}_{t=1}^{\hat{M}} \underset{\text{sensing}}{\overset{\text{collaborative}}{\longrightarrow}} \left\{\left(\hat{\boldsymbol{\theta}}_t^{'}, \hat{\boldsymbol{J}}_{\boldsymbol{\theta}_t^{'}}\right)\right\}_{t=1}^{\hat{M}} \overset{\{\boldsymbol{\theta}_a\}}{\longrightarrow} \boldsymbol{T} \overset{\mathcal{D}=\emptyset}{\longrightarrow} \hat{s}_b^*. \tag{26}$$

The proposed MIFTP estimation technique provides an approximate upper bound on the transmit power of a secondary transmitter. The construction, sharing, and updating of the T-map throughout the network is an integral part of our approach, because in addition to quantifying the spectrum holes, the use of collaboration makes the scheme adaptive and robust. In ongoing work, we are studying the parameters that the T-map requires to successfully characterize the spectrum holes in dynamic scenarios, as well as the associated networking issues.

Appendix

A. CRB of $\hat{\boldsymbol{\theta}}_{1B}$ and $\hat{\boldsymbol{\theta}}_{1C}$

Suppose there are M cochannel primary transmitters. The scaled observations conditioned on all the parameters can be modeled as (cf. Section III-B)

$$\widetilde{R}_a | \{\boldsymbol{\theta}_i\}_{i=1}^{M} \sim \mathcal{N}\left(\ln\left(\sum_{i=1}^{M} e^{\kappa u_{a p_i}}\right), \kappa^2 \sigma_W^2\right). \tag{27}$$

Given the set of independent observations $\widetilde{\mathcal{O}}_1 \triangleq \left\{(\widetilde{R}_a, \boldsymbol{L}_a) : a \in \mathcal{A}_1\right\}$ and known parameters $\{\boldsymbol{\theta}_i\}_{i=2}^{M}$, we are interested in calculating the CRB, $\boldsymbol{J}_{\boldsymbol{\theta}_{1B}}^{-1}$, corresponding to estimator $\hat{\boldsymbol{\theta}}_{1B}$. The Fisher Information

matrix (FIM) is given by

$$\boldsymbol{J}_{\boldsymbol{\theta}_{1B}} \equiv \boldsymbol{J}_{\boldsymbol{\theta}_1|\{\boldsymbol{\theta}_i\}_{i=2}^M} = E_{\{\boldsymbol{\theta}_i\}_{i=1}^M}\left[\left(\frac{\partial l(\boldsymbol{\theta}_1)}{\partial \boldsymbol{\theta}_1}\right)\left(\frac{\partial l(\boldsymbol{\theta}_1)}{\partial \boldsymbol{\theta}_1}\right)^T\right], \tag{28}$$

where $E_{\{\boldsymbol{\theta}_i\}_{i=1}^M}[\cdot]$ denotes conditional expectation with respect to $\{\boldsymbol{\theta}_i\}_{i=1}^M$. $l(\boldsymbol{\theta}_1)$ represents the log-likelihood function, which can be written as

$$l(\boldsymbol{\theta}_1) = \sum_{a\in\mathcal{A}_1} \ln f_{\widetilde{R}_a|\{\boldsymbol{\theta}_i\}_{i=1}^M}(\widetilde{R}_a), \tag{29}$$

where $f_{\widetilde{R}_a|\{\boldsymbol{\theta}_i\}_{i=1}^M}(\cdot)$ denotes the probability density function of $\widetilde{R}_a|\,\{\boldsymbol{\theta}_i\}_{i=1}^M$. Using (27)-(29), it is simple to verify that $\boldsymbol{J}_{\boldsymbol{\theta}_{1B}} = \frac{1}{\sigma_W^2}\sum_{a\in\mathcal{A}_1} k_a \boldsymbol{G}_a \boldsymbol{G}_a^T$, where

$$\boldsymbol{G}_a \triangleq \begin{bmatrix} \dot{g}(d_{ap_1})\cos\phi_{ap_1} & \dot{g}(d_{ap_1})\sin\phi_{ap_1} & -1 \end{bmatrix}^T, \quad k_a \triangleq \frac{e^{\kappa u_{ap_1}}}{\sum_{i=1}^M e^{\kappa u_{ap_i}}} \leq 1. \tag{30}$$

For the case of $\hat{\boldsymbol{\theta}}_{1C}$, the scaled observations can be modeled as (cf. Section III-C)

$$\widetilde{R}_a|\boldsymbol{\theta}_1, \{\hat{\boldsymbol{\theta}}_i\}_{i=2}^M \sim \mathcal{N}\left(\ln\left(\sum_{i=1}^M e^{\kappa u_{ap_i} + \frac{\kappa^2\hat{\sigma}_{ia}^2}{2}}\right), \kappa^2\sigma_W^2\right), \tag{31}$$

where $\hat{\sigma}_{ia}^2 \triangleq \hat{\boldsymbol{G}}_a \hat{\boldsymbol{J}}_{\boldsymbol{\theta}_i}^{-1} \hat{\boldsymbol{G}}_a^T$ with $\hat{\sigma}_{1a}^2 \triangleq 0$. Recall that in our notation $\hat{\boldsymbol{A}}$ denotes the MLE of $\boldsymbol{A}$. As before, we have $\boldsymbol{J}_{\boldsymbol{\theta}_{1C}} = \frac{1}{\sigma_W^2}\sum_{a\in\mathcal{A}_1} m_a \boldsymbol{G}_a \boldsymbol{G}_a^T$, where

$$m_a \triangleq \frac{e^{\kappa u_{ap_1}}}{\sum_{i=1}^M e^{\kappa u_{ap_i} + \frac{\kappa^2\hat{\sigma}_{ia}^2}{2}}} \leq k_a \leq 1. \tag{32}$$

If no information is available about the multiple cochannel transmitters (cf. Section III-A), then the net SS can be assumed to result from a single *virtual transmitter*. Interestingly, the FIM corresponding to the virtual transmitter $V \equiv p_1$ is given by $\boldsymbol{J}_{\boldsymbol{\theta}_V} = \frac{1}{\sigma_W^2}\sum_{a\in\mathcal{A}_1} \boldsymbol{G}_a \boldsymbol{G}_a^T$. It is easy to show that $\boldsymbol{J}_{\boldsymbol{\theta}_{1C}}^{-1} \geq \boldsymbol{J}_{\boldsymbol{\theta}_{1B}}^{-1} \geq \boldsymbol{J}_{\boldsymbol{\theta}_V}^{-1}$, where $\boldsymbol{Y} \geq \boldsymbol{Z}$ should be interpreted to mean that $\boldsymbol{Y} - \boldsymbol{Z}$ is non-negative definite. Similar to the single transmitter case, from (27) and (31) we conclude that the above CRBs will be achievable asymptotically as $\sigma_W \to 0$.

B. Proof of Proposition 1

The interference caused to v located at $(x_v, y_v) \in \overline{B}_{\text{cov}}(p)$ due to all secondary transmissions is given by $I_v = 10\log_{10}\left(\sum_{a\in\mathcal{A}_0} 10^{\frac{I_{va}}{10}}\right)$, where $I_{va} = s_a - g(d_{va}) + W_{va}$ and $W_{va} \sim \mathcal{N}(0, \sigma_W^2)$, $\forall a \in \mathcal{A}_0$. Similar to Section III, given $\boldsymbol{\Theta}$, I_v can be modeled as $I_v \sim \mathcal{N}(\frac{\mu}{\kappa}, \frac{\sigma^2}{\kappa^2})$. So the interference probability $P_{\text{int}}(\mathcal{A}_0; s_b, v)$ is given by

$$P_{\text{int}}(\mathcal{A}_0; s_b, v) \triangleq \Pr(I_v \geq i_{\max}) = Q\left(\frac{i_{\max} - \frac{\mu}{\kappa}}{\frac{\sigma}{\kappa}}\right) \overset{(15)}{=} Q\left(\frac{\kappa i_{\max} - \frac{\kappa^2\sigma_W^2}{2} + \frac{\sigma^2}{2} - h}{\sigma}\right). \tag{33}$$

C. Proof of Proposition 2

Suppose $g(d) = 10\epsilon \log_{10}(d)$. Let I_v be the interference power at an arbitrary victim node v located at $(x_p + r_0 \cos\psi, y_p + r_0 \sin\psi)$ where $r_0 < d_{\text{cov}}(p)$, (see Fig. 3a). There exists a particular victim node $\tilde{v}$ located at $(x_p + r_0 \cos\tilde{\psi}, y_p + r_0 \sin\tilde{\psi})$, such that $I_v \leq I_{\tilde{v}}$. Choose $(x_p + r_0 \cos\tilde{\psi}, y_p + r_0 \sin\tilde{\psi})$ as the new origin (see Fig. 3b), and denote the shortest straight line connecting this origin to $\partial B_{\text{cov}}(p)$ as l. Then the aggregate interference power (in absolute scale) at any point $(r, 0)$ on l is given by

$$I_l = \sum_{a \in \mathcal{A}_T} \frac{10^{\frac{s_a}{10}}}{[(\tilde{x}_a - r)^2 + \tilde{y}_a^2]^{\frac{\epsilon}{2}}}, \tag{34}$$

where $(\tilde{x}_a, \tilde{y}_a)$ is the location of secondary transmitter a with respect to the new origin. The value of I_l will monotonically increase with increasing r, since it points to the direction of the stronger interferers. This is because, staying on l as we move towards the edge, we move towards the stronger interferers and move away from the weaker ones, and as a result, the increase in interference due to the stronger interferers will offset the decrease in interference due to the weaker interferers. Therefore, we can always start at an arbitrary interior point of $\overline{B}_{\text{cov}}(p)$ and reach a point on its circumference where the interference is greater. The conclusion continues to hold for different path loss functions $g(d)$ that are monotonically increasing.

D. Proof of Corollary 1

Consider an arbitrary victim node v located at $(x_p + r\cos\psi, y_p + r\sin\psi) \in \overline{B}_{\text{cov}}(p)$, where $(r, \psi) \in (0, d_{\text{cov}}(p)] \times [0, 2\pi) \triangleq \mathcal{F}_1 \times \mathcal{F}_2$. Let $i_v(r, \psi, s_b)$, parameterized in the 3-tuple (r, ψ, s_b), denote the aggregate interference power at v (in absolute scale) without any shadowing noise, W. We can upper bound the interference probability as follows.

$$\begin{aligned}
\text{P}_{\text{int}}(\mathcal{A}_0; s_b, v) &\triangleq \Pr(I_v \geq i_{\max}) \\
&= \Pr\left(i_v(r, \psi, s_b) \cdot 10^{\frac{W}{10}} \geq 10^{\frac{i_{\max}}{10}}\right) \\
&\leq \Pr\left(10^{\frac{W}{10}} \geq \frac{10^{\frac{i_{\max}}{10}}}{\max\limits_{(r,\psi) \in \mathcal{F}_1 \times \mathcal{F}_2} i_v(r, \psi, s_b)}\right) \\
&\overset{\text{Prop.2}}{=} \Pr\left(10^{\frac{W}{10}} \geq \frac{10^{\frac{i_{\max}}{10}}}{i_v(d_{\text{cov}}(p), \psi^*, s_b)}\right),
\end{aligned} \tag{35}$$

for a particular ψ^*. Since (35) is an upper bound on $\mathrm{P}_{\text{int}}(\mathcal{A}_0; s_b, v)$, for MIFTP computation, we can fix $r = d_{\text{cov}}(p)$ and it is sufficient to restrict the search to $\psi \in [0, 2\pi)$.

E. Proof of Proposition 3

From the definition of h in (15) we have

$$\begin{aligned} e^{2h} &= L_b^2 + L_T^2 + 2L_bL_T > L_b^2 + L_T^2 \\ \Leftrightarrow e^{\kappa^2\sigma_W^2} - 1 &> e^{-2h}\left(e^{\kappa^2\sigma_W^2} - 1\right)\left(L_b^2 + L_T^2\right) \overset{(16)}{=} \frac{k_6^2}{k_5^2} \\ \Leftrightarrow \kappa^2\sigma_W^2 &> \ln\left(1 + \frac{k_6^2}{k_5^2}\right) \overset{(15)}{=} \sigma^2. \end{aligned} \tag{36}$$

Consider the interference probability:

$$P_{\text{int}}(\mathcal{A}_0; s_b, v) \overset{(14)}{=} Q\left(\frac{\kappa i_{\max} - \frac{\kappa^2\sigma_W^2}{2} + \frac{\sigma^2}{2} - h}{\sigma}\right) \overset{(36)}{\leq} Q\left(\frac{\kappa i_{\max} - \frac{\kappa^2\sigma_W^2}{2} + \frac{\sigma^2}{2} - h}{\kappa\sigma_W}\right) = Q(\gamma). \tag{37}$$

F. Value of $\boldsymbol{H}_0$

Define the following terms:

$$c_1 \triangleq \left(\kappa\sigma_W(k_5^2 + k_6^2)\right)^{-1},\ c_2 \triangleq e^{\kappa^2\sigma_W^2}\left(e^{\kappa^2\sigma_W^2} - 1\right),\ c_3 \triangleq \left(k_5^2 + 2k_6^2\right)e^{-h}. \tag{38}$$

It can be verified that $\boldsymbol{H}_0 = -\kappa c_1\left(\left(c_2L_b - c_3\right)\boldsymbol{H}_b + \sum_{a\in\mathcal{A}_T}\left(c_2L_a - c_3\right)\boldsymbol{H}_a\right)$, where

$$\boldsymbol{H}_b \triangleq L_b\dot{g}(d_{vb})\begin{bmatrix} \cos\phi_{vb} \\ \sin\phi_{vb} \\ -\dot{d}_{\text{cov}}(p) \end{bmatrix}, \quad \boldsymbol{H}_a \triangleq L_a\dot{g}(d_{va})\begin{bmatrix} \cos\phi_{va} - \frac{d_{\text{cov}}(p)}{d_{bp}}\sin\phi_{bp}\sin(\phi_{bp} - \phi_{va}) \\ \sin\phi_{va} + \frac{d_{\text{cov}}(p)}{d_{bp}}\cos\phi_{bp}\sin(\phi_{bp} - \phi_{va}) \\ \dot{d}_{\text{cov}}(p)\cos(\phi_{bp} - \phi_{va}) \end{bmatrix},$$

with $\phi_{ij} \triangleq \tan^{-1}\left(\frac{y_i - y_j}{x_i - x_j}\right)$, $\dot{g}(d) \triangleq \frac{\partial g(d)}{\partial d}$ and $\dot{d}_{\text{cov}}(p) \triangleq \frac{\partial d_{\text{cov}}(p)}{\partial s_p}$.

REFERENCES

[1] S. Haykin, "Cognitive radio: Brain-empowered wireless communications," *IEEE J. Selected Areas in Comm.*, vol. 23, pp. 201–220, Feb. 2005.

[2] Q. Zhao and B. M. Sadler, "A survey of dynamic spectrum access," *IEEE Signal Proc. Mag.*, vol. 24, pp. 79–89, May '07.

[3] C. Raman *et al.*, "Scheduling variable rate links via a spectrum server," in *Proc. IEEE DySPAN*, pp. 110–118, Nov. 2005.

[4] N. Devroye *et al.*, "Achievable rates in cognitive radio," *IEEE Trans. Info. Theory*, vol. 52, pp. 1813–1827, May 2006.

[5] R. Etkin *et al.*, "Spectrum sharing for unlicensed bands," in *Proc. IEEE DySPAN*, pp. 251–258, Nov. 2005.

[6] S. Tang and B. L. Mark, "Modeling and analysis of opportunistic spectrum sharing with unreliable spectrum sensing," *IEEE Trans. Wireless Commun.*, 2008. accepted.

[7] Y. Chen, Q. Zhao, and A. Swami, "Joint Design and Separation Principle for Opportunistic Spectrum Access in the Presence of Sensing Errors," *IEEE Trans. on Information Theory*, vol. 54, pp. 2053–2071, May 2008.

[8] A. Ghasemi and E. Sousa, "Collaborative spectrum sensing for opportunistic access in fading environments," in *Proc. IEEE Int. Symp. on New Frontiers in Dynamic Spectrum Access Networks (DySPAN)*, pp. 131–136, Nov. 2005.

[9] G. Ganesan and L. Ye, "Cooperative Spectrum Sensing in Cognitive Radio, Part I: Two User Networks," *IEEE Trans. on Wireless Communications*, vol. 6, pp. 2204–2213, June 2007.

[10] A. Sahai and N. Hoven and S. M. Mishra and R. Tandra, "Fundamental tradeoffs in robust spectrum sensing for opportunistic frequency reuse," tech. rep., University of California, Berkeley, March 2006.

[11] H. Celebi and H. Arslan, "Utilization of location information in cognitive wireless networks," *IEEE Wireless Commun. Mag.*, vol. 14, pp. 6–13, Aug. 2007.

[12] H. Celebi and H. Arslan, "Cognitive Positioning Systems," *IEEE Trans. on Wireless Communications*, vol. 6, pp. 4475–4483, Dec. 2007.

[13] S. Kim and H. Jeon and J. Ma, "Robust localization with unknown transmission power for cognitive radio," in *Proc. IEEE MILCOM'07*, Oct. 2007.

[14] J. Nelson *et al.*, "Global Optimization for Multiple Transmitter Localization," in *IEEE MILCOM'06*, pp. 1–7, Oct. 2006.

[15] J. Nelson and M. R. Gupta, "An EM technique for multiple transmitter localization," in *CISS'07*, pp. 610–615, Mar. 2007.

[16] C. Raman *et al*, "Distributed Spatio-Temporal Spectrum Sensing: An Experimental Study," in *Proc. Asilomar conference on Signals, Systems, and Computers*, (Pacific Grove, CA), pp. 2063–2067, Nov. 2007. (invited paper).

[17] R. Chen, J. M. Park, and J. H. Reed, "Defense against primary user emulation attacks on cognitive radio networks," *IEEE Trans. Selected Areas in Commun.*, vol. 26, pp. 25–37, Jan. 2008.

[18] P. Mahonen, M. Petrova, and J. Riihijarvi, "Applications of Topology Information for Cognitive Radios and Networks," in *Proc. IEEE DySPAN*, pp. 103–114, Apr. 2007.

[19] L.-C. Wang and A. Chen, "Effects of Location Awareness on Concurrent Transmissions for Cognitive Ad Hoc Networks Overlaying Infrastructure-based Systems," *IEEE Trans. on Mobile Computing*, 2008. Accepted for publication.

[20] L. Qian, X. Li, J. Attia, and Z. Gajic, "Power control for cognitive radio ad hoc networks," in *Proc. 15th IEEE Workshop on LANMAN*, (NJ, U.S.A.), pp. 7–12, June 2007.

[21] K. Hamdi and W. Zhang and K. B. Letaief, "Power Control in Cognitive Radio Systems Based on Spectrum Sensing Side Information," in *Proc. IEEE ICC*, pp. 5161–5165, June '07.

[22] A. E. Leu, M. McHenry, and B. L. Mark, "Modeling and analysis of interference in Listen-Before-Talk spectrum access schemes," *Int. J. Network Mgmt*, vol. 16, pp. 131–147, 2006.

[23] B. L. Mark and A. O. Nasif, "Estimation of Interference-Free Transmit Power for Opportunistic Spectrum Access," in *Proc. IEEE Wireless Communications and Networking Conference (WCNC'08)*, pp. 1679–1684, Apr. 2008.

[24] B. L. Mark and A. E. Leu, "Local averaging for fast handoffs in cellular networks," *IEEE Trans. Wireless Commun.*, vol. 6, pp. 866–874, March 2007.

[25] N. C. Beaulieu *et al.*, "Estimating the distribution of a sum of independent lognormal random variables," *IEEE Trans. on Comm.*, vol. 43, pp. 2869–2873, Dec. 1995.

[26] L. L. Scharf, *Statistical Signal Processing: Detection, Estimation, and Time Series Analysis*. NY: Addison-Wesley, 1991.

[27] B. L. Mark and A. O. Nasif, "Estimation of Interference-Free Power for Opportunistic Spectrum Access," tech. rep., George Mason University, Aug. 2008. Available at $http://napl.gmu.edu/pubs/TReports/MarkNasif\_miftp-tr08.pdf$.

[28] A. O. Nasif and B. L. Mark, "Opportunistic spectrum access with multiple transmitters," Tech. Rep. TR-GMU-NAPL-Y09-N1, George Mason University, Feb. 2009. Available at http://napl.gmu.edu.

[29] A. O. Nasif and B. L. Mark, "Measurement clustering criteria for localization of multiple transmitters," in *Proc. Conf. Info. Sciences and Systems (CISS'09)*, (Baltimore, MA), Mar. 2009 (to appear).

[30] J. Rissanen, "Modeling by shortest data description," *Automatica*, vol. 14, pp. 465–471, 1978.

[31] S. Verdú, *Multiuser Detection*. New York: Cambridge University Press, 1998.

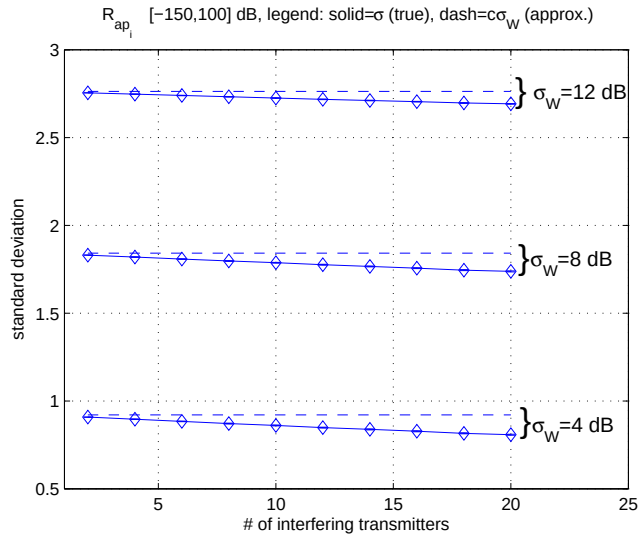

Fig. 1. Plot shows the mean values of σ_{Ba}, calculated according to (9)-(10), with the associated 99.7% confidence intervals generated from 10^4 random realizations of $u_{ap_i} \in [-150, 100]$ dB, $\forall p_i \in \mathcal{P}$, where $|\mathcal{P}| \in [2, 20]$.

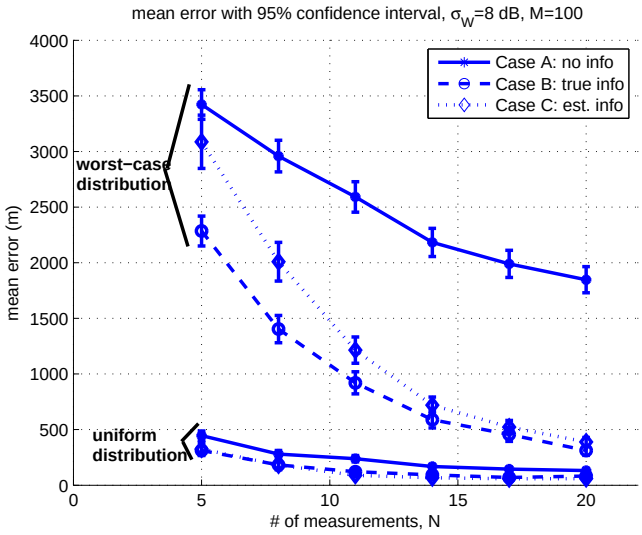

Fig. 2. Localization error $\mathcal{E}_1$ vs. number of measurements.

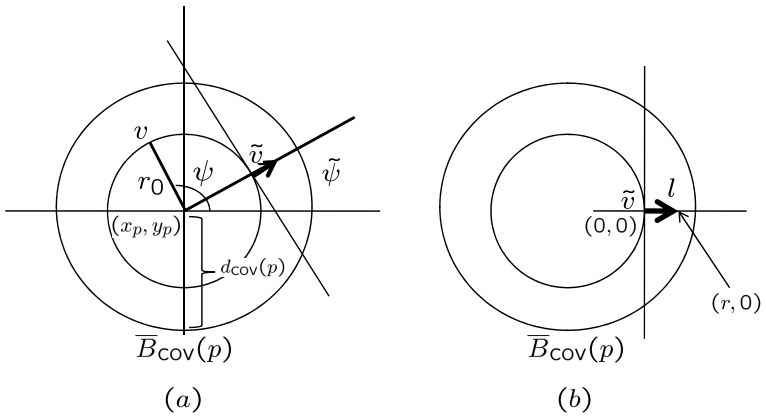

Fig. 3. Diagram for the proof of Proposition 2. In (a), node v located at $(x_p + r_0 \cos\psi, y_p + r_0 \sin\psi) \in \overline{B}_{\mathrm{cov}}(p)$ represents an arbitrary victim. There exists a node $\tilde{v}$ at angle $\tilde{\psi}$ located at $(x_p + r_0 \cos\tilde{\psi}, y_p + r_0 \sin\tilde{\psi})$, such that $I_v \leq I_{\tilde{v}}$. In (b), the location of $\tilde{v}$ is chosen as the new origin. Because of the way the angle $\tilde{\psi}$ is chosen, the interference on the line l is monotonically increasing in r.

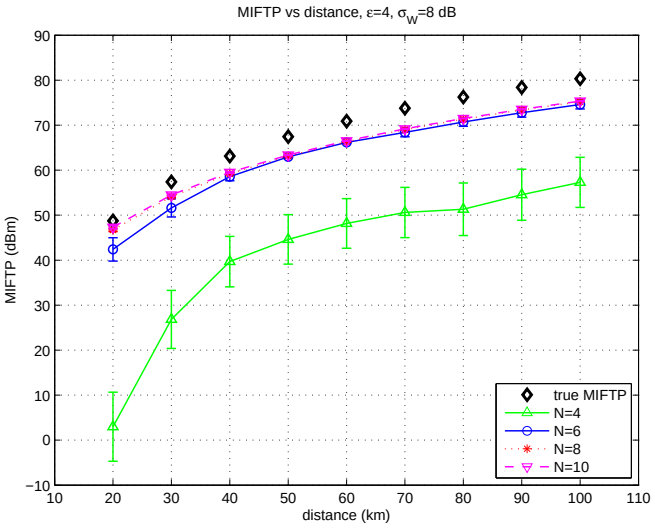

Fig. 4. MIFTP vs d_{bp}, for single primary transmitter p.

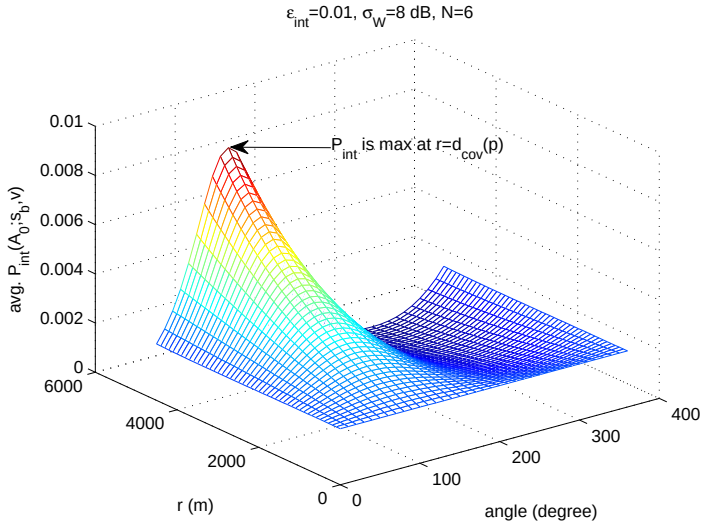

Fig. 5. Average interference probability surface due to $\hat{s}_b^*(p)$ in the coverage region $\overline{B}_{\rm cov}(p)$.

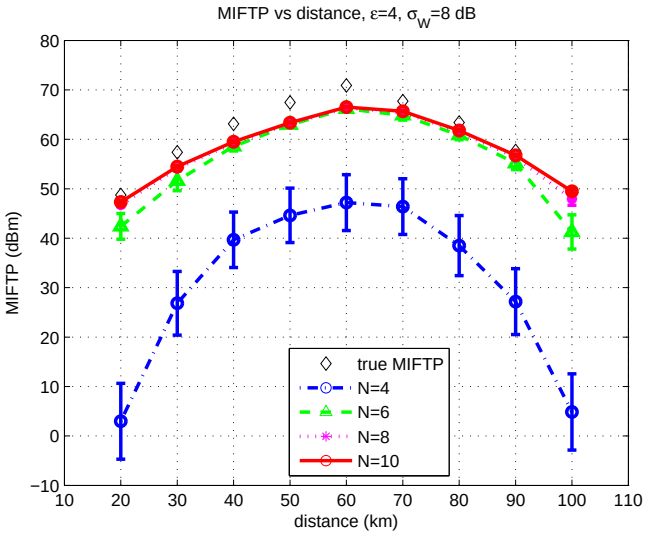

Fig. 6. MIFTP vs d_{bp}, for two primary transmitters, p and $p^{'}$.

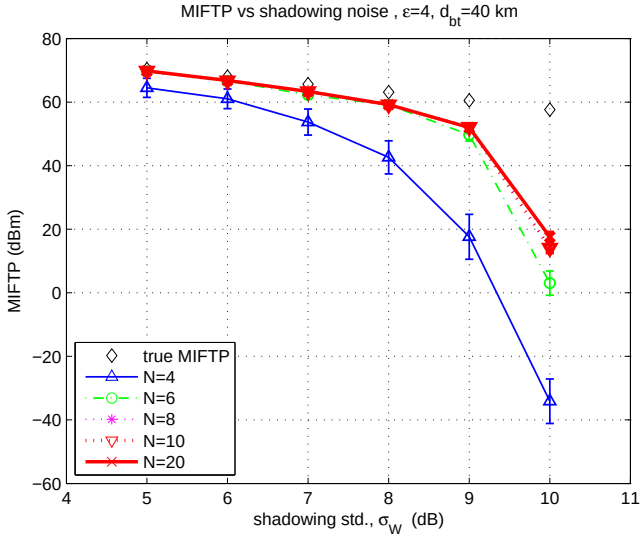

Fig. 7. MIFTP vs shadowing noise, σ_W.

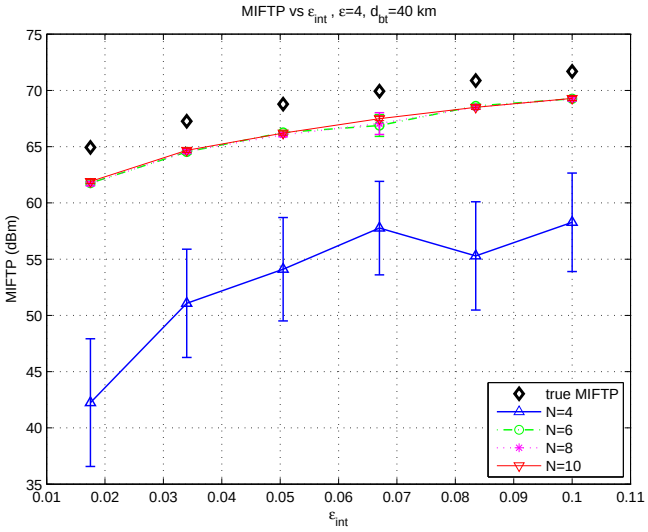

Fig. 8. MIFTP vs maximum interference probability threshold, ε_{int}.

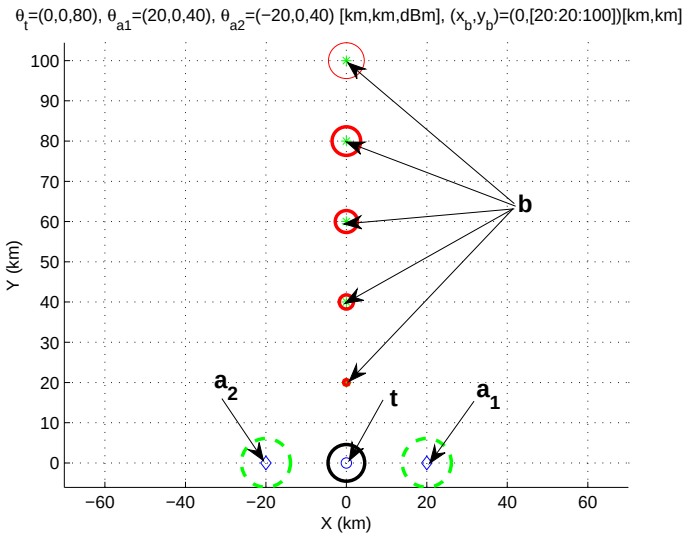

Fig. 9. Pictorial illustration of a T-map and spectrum hole harvesting in space.